Eurasian Journal of Physics and Functional Materials

Volume 8 | Number 3

Article 4

Pages: 122 - 130

2024

Investigations on the Growth and Optical, Dielectric and Antibacterial activity of L-Leucine Barium Chloride crystals

M. Arul Tresa
Research Scholar, (Reg.No. 18221282132038), PG and Research Department of Physics, St. Xavier's College (Autonomous), Palayamkottai- 627002, Tirunelveli, Tamilnadu, India, tresapaul.kk@gmail.com

B. Helina
PG and Research Department of Physics, St. Xavier's College (Autonomous), Palayamkottai - 627002, Tirunelveli, Tamilnadu, India

S. C. Vella Durai
PG and Research Department of Physics, Sri Paramakalyani College, Alwarkurichi -627412, Tenkasi, Tamilnadu, India

Recommended Citation

Tresa, M. Arul; Helina, B.; and Durai, S. C. Vella (2024) "Investigations on the Growth and Optical, Dielectric and Antibacterial activity of L-Leucine Barium Chloride crystals," *Eurasian Journal of Physics and Functional Materials*: Vol. 8: No. 3, Article 4.
DOI: https://doi.org/10.69912/2616-8537.1227

ORIGINAL STUDY

Investigations on the Growth and Optical, Dielectric and Antibacterial Activity of L-leucine Barium Chloride Crystals

M. Arul Tresa [a,*], B. Helina [a], S.C. Vella Durai [b]

[a] PG and Research Department of Physics, St. Xavier's College (Autonomous), Palayamkottai, 627002, Tirunelveli, Tamilnadu, India
[b] PG and Research Department of Physics, Sri Paramakalyani College, Alwarkurichi, 627412, Tenkasi, Tamilnadu, India

Abstract

In order to create single crystal of L-Leucine Barium Chloride (LLBC), double-distilled water was utilized as solvent in a solution strategy with a lengthy evaporation process. L-Leucine and Barium Chloride, both of which are of AR quality, were bought commercially and consumed in an equal amount. By slow evaporation method single crystals were formed after a period of about 30 days. Solubility tests for the crystal were carried out, and it was observed that solubility increases with temperature. Single crystal X-ray diffraction (XRD) was used to carry out the XRD test to determine the crystal structure of the material and it was found to be orthorhombic. The sample's SHG effectiveness was found using Nd:YAG laser and green laser light was produced by the crystal. A microhardness tester was used to find the mechanical parameters of LLBC crystals, the hardness, work hardening coefficient, yield strength, stiffness constant, resistance pressure, fracture toughness, and brittleness index, have been evaluated to understand the sample's mechanical strength. Following the sample's linear optical exams, numerous linear optical properties of the sample have been computed. The antibacterial activity of four bacterial strains was studied to understand the prevention of the bacterial growth.

Keywords: Hardness, NLO, Transmittance, Optical conductivity, Single crystal, Solution growth, XRD, SHG, Antibacterial activity

1. Introduction

NLO crystals are employed in numerous industries, such as optical communication, optical computing, and optoelectronics [1,2]. Organic, inorganic, or semiorganic non linear optical (NLO) crystals are commonly categorised. NLO crystals each have their own benefits and drawbacks. High NLO efficiency, adaptable molecular structure, and innately short response time are all characteristics of organic NLO crystals. Inorganic NLO crystals are more mechanically robust, more thermally stable, and less effective than organic NLO crystals [3—6]. Due to its intermediate mechanical strength and thermal stability compared to organic and inorganic NLO crystals, a semiorganic NLO crystal called L-leucine barium chloride is created and examined here. Soma Adhikari and colleagues have cultivated and studied L-leucine [7] and it is a crucial amino acid. "According to reports, L-Leucine has been combined with nitric acid, oxalic acid, perchloric acid, and picric acid to produce a number of compounds that have been found to be useful NLO materials" [8—11]. Jagadeesh and colleagues synthesized L-leucine phthalic acid potassium iodide by mixing L-leucine, phthalic acid, and potassium iodide in a 1:1:1 molar ratio, followed by formation from an aqueous solution through slow evaporation. Various analyses, including single crystal XRD, FTIR, UV-Vis, TGA, SEM, EDAX, microhardness, dielectric, and powder SHG assessments, were conducted on these crystals. The findings from these analyses of the produced L-Leucine Phthalic acid

Received 28 May 2024; revised 7 September 2024; accepted 10 September 2024.
Available online 19 October 2024

* Corresponding author at: Affiliated to Manonmaniam Sundaranar University, Tirunelveli, 627012, Tamilnadu, India.
E-mail address: tresapaul.kk@gmail.com (M. Arul Tresa).

https://doi.org/10.69912/2616-8537.1227

Potassium Iodide crystals have been examined [12]. Baskaran et al., employed the solvent evaporation method at room temperature to produce a single crystal of L-Leucinium Perchlorate. Single crystal XRD analysis revealed a monoclinic structure of the generated crystals. Additionally, infrared Fourier transform spectrum analysis and UV-vis spectral studies were conducted. The microhardness study indicated a decrease in crystal hardness under stress. Analysis using the Kurtz and Perry powder method for nonlinear optical properties showed a second harmonic generation efficiency 2.6 times higher than that of KDP crystals [13]. From a crystal engineering perspective, L-Leucine is recognized as one of the amino acid molecules. L-Leucine based crystals have attracted a lot of interest due to their exceptional NLO properties [10,14−17]. L-leucinium oxalate crystals were generated by Anbuchezhiyan et al. and described by numerous research [18]. L-leucinium oxalate single crystals have been produced and examined by Bhaskaran and colleagues [19]. L-leucine hyrobromide crystals have been produced and investigated by Adhikari et al. and Subramanian [20,21]. L-leucine has reportedly been employed in both supramolecular research and crystal engineering, and certain L-leucine-based NLO crystals have been documented in the literature [22−25]. L-leucine and barium chloride were combined to create a single crystal of LLBC, a semiorganic NLO crystal, in this study. This study examines the structural, NLO, bactericidal, and mechanical characteristics of the LLBC crystal and the results are presented.

2. Materials and methods

L-Leucine Barium Chloride is a mixer of L-Leucine and Barium Chloride with 1:1 molar ratio of analytical reagent (AR) grade chemicals (LLBC). The calculated amount of L-Leucine and Barium Chloride were thoroughly mixed with double-distilled water using a magnetic stirrer and allowed to stand for around 3 h. The solution was heated to produce salt of LLBC. The temperature of the solution was maintained at 50 °C during the synthesis. The solubility of the material was determined gravimetrically and Fig. 1 shows the solubility curve of LLBC. It has been revealed that LLBC becomes more soluble as temperature increases. The solubility curve was used to create the saturated solution, which was then constantly stirred for 2 h using a magnetic stirrer before filtering through four mico Whatmann filter sheets. The filtered mixture was then kept in a dust-free environment in a Borosil beaker that was wrapped in porous paper. The extraction of the crystals took about 30 days. A high-quality LLBC crystal was grown and it is shown in Fig. 2.

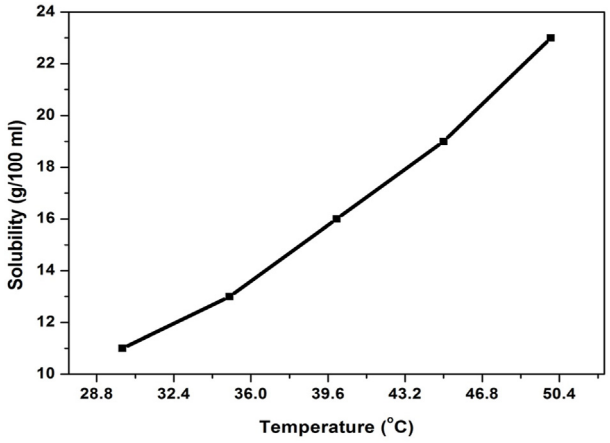

Fig. 1. Solubility curve of LLBC crystal.

Fig. 2. Photograph of grown LLBC crystal.

3. Results and discussions

3.1. X-ray diffraction (XRD) analysis

The X-ray diffraction analysis of LLBC was conducted using a diffractometer. The crystallographic parameters obtained were: a = 12.254 (2) Å, b = 6.538 (4) Å, c = 8.375 (2) Å, $\alpha = 90^\circ$, $\beta = 90^\circ$, $\gamma = 90^\circ$. These data indicate that the crystal adopts an orthorhombic structure. The unit cell volume of the crystal was determined to be 670.98 Å.

3.2. Second harmonic generation (SHG) studies

The nonlinear optical properties of the fabricated LLBC were assessed using the Kurtz and Perry technique [26]. A Q-switched Nd:YAG laser with a fundamental wavelength of 1064 nm from the Quanta ray series served as the light source. The sample material was ground into a powder and tightly packed into a small capillary tube. The incident beam's power was

measured using a power meter. For the second harmonic generation (SHG) measurement, KDP crystals crushed to a similar size as the LLBC sample were used as reference material. The powdered LLBC sample was exposed to a laser beam with an input energy of 0.71 J, resulting in second harmonic signal energy of 9.5 mJ. In comparison, the reference KDP sample generated SHG signal energy of 8.8 mJ under identical input beam energy. Consequently, the SHG efficiency of the LLBC crystal is 1.07 times greater than that of KDP.

3.3. Mechanical properties

Micro hardness experiments were conducted to investigate the mechanical characteristics of LLBC crystals. The testing was performed with a Shimadzu Vickers Microhardness Tester, which was outfitted with a diamond indenter and a reflected light microscope. The crystals were supported on a Vickers Microhardness testing platform under various loads of varying intensities. After measuring both diagonal indentation values, we determined the average indentation value. Fig. 3 shows the relationship between the stress of the LLBC crystal and the standard value of the diagonal notch (d). It is clear that the average diagonal indentation value (d) of LLBC crystals increases with increasing load. "The microhardness number was calculated using the equation $H_v = 1.8544\ P/d2$, where P is the applied load (H_v)" [27]. The microhardness number of the sample are shown in Fig. 4 as a function of the applied load. The results shows that the hardness number increases with increasing applied load. The increasing trend of the plot is due to the reverse indentation size effect. When a low load is applied, the sample first gets tougher, making it able to withstand higher stresses. This is what causes the LLBC crystal to get harder as load is applied to it. Higher loads have the tendency to induce the value of H_v to saturate, and significant cracking at a load of 100 g may result from

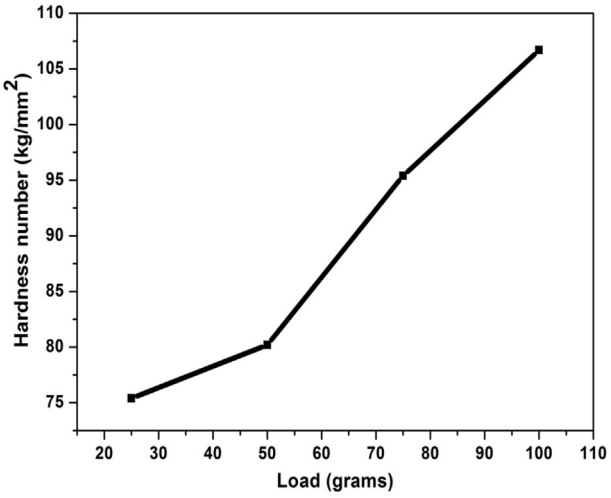

Fig. 4. Hardness number vs applied load.

the release of locally generated internal stresses via indentation [28].

Meyer's law defines the relationship P = k1 dn, where n represents Meyer's index, also termed as the work hardening coefficient, and k1 denotes the material constant. By logarithmically transforming both sides, one obtains log P = log k1 + n log d. This equation forms a straight line with a slope of n. Fig. 5 illustrates the log (P) against log plot. Through the best linear fit, the work hardening coefficient (n) is estimated from this plot, yielding a value of 2.873. The behavior of the standard indentation size effect (ISE) occurs when the work hardening coefficient (n) is less than two, while the reverse indentation size effect (RISE) manifests when n exceeds two. Thus, since n is greater than 2, LLBC crystal exhibits the RISE effect, indicating it belongs to the category of soft materials [29,37].

The Hays-Kendall method can be used to provide mechanical parameters such corrected indentation size

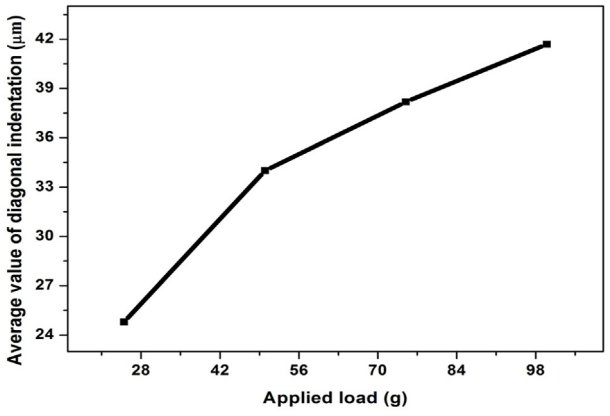

Fig. 3. Applied load vs the average diagonal indentation value.

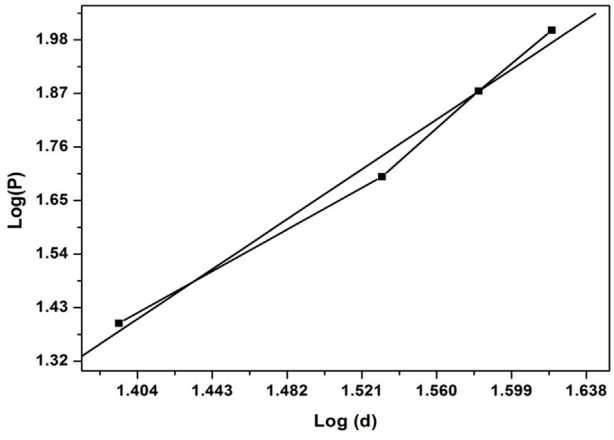

Fig. 5. log (P) vs log (d) for LLBC.

independent hardness, resistance pressure, and plastic deformation. The Hays-Kendall formula, expressed as P═W + Adˆ2, defines the relationship between the applied load (P), the load-independent constant (A), and the average diagonal indentation length (d). Here, W represents the minimal force needed to initiate plastic deformation. Fig. 6 illustrates the plot between P and d̂2, where the values of W and A are determined. Notably, the LLBC crystal displays the reverse indentation size effect, as evidenced by the negative value of W (−19.691 g). The microhardness number (Ho) is calculated using the relation Ho = 1.8544 A, with a slope value of A = 0.0662 g/m̂2 obtained from the graph. For the LLBC crystal, Ho was computed to be 0.123 g/m̂2 [30,31].

"Fracture toughness is the relative level of impact resistance where there is no material fracture. In other words, the material can withstand stress over its breaking point while still absorbing energy". The fracture mechanics of the indentation process offer an equilibrium relation for a well-established crack expanding under central loading conditions. Indentation-induced fractures may manifest as either radial-median cracks or Palmqvist cracks. The fracture toughness (K_c) can be determined using the following relationship.

$$K_c = \frac{P}{\beta_0 c^{3/2}}$$

where $\beta_o = 7$ for the Vickers hardness indenter, P is the applied stress, c is the length of the indentation formed by the crack, and c is 37 μm for a 100 g weight. The predicted fracture toughness of LLBC is 0.063 g/(μm)$^{3/2}$. Brittleness, which determines whether a crystal will shatter without considerably deforming, is another important characteristic of crystals from a mechanical perspective. The brittleness index (Bi) is used to quantify brittleness and is reported as

$$B_i = \frac{H_v}{K_c}$$

In that situation, H_v is the Vickers hardness number. The LLBC crystal's Brittle index is determined to be 1.698 μm$^{-1/2}$ with an applied force of 100 g [32].

Mechanical parameters such as yield strength and stiffness constant can be derived from microhardness and work hardening coefficient values. Yield strength represents the maximum stress a material can endure before undergoing plastic deformation. The relationship between microhardness (H_v) and work hardening coefficient (n), which determine yield strength, is expressed as yield strength (σ_y) = (H_v/3)(0.1) n-1/2. The stiffness constant (C_{11}) is calculated using the formula C_{11}= Hv̂7/4, where Hv denotes the microhardness of the crystal. Fig. 7 illustrates the relationship between the load and yield strength, as well as the stiffness constant for the LLBC crystal. The findings indicate that both yield strength and stiffness constant increase with the applied load.

3.4. Linear optical studies

Due to the low intensity, UV and visible light that was used to record the spectrum, this work is referred to as a linear optical survey. The linear optical properties are primarily influenced by factors such as optical transparency, absorption coefficient, band gap, extinction coefficient, and refractive index. The interaction of the crystal with the electric and magnetic fields of electromagnetic waves dictates its optical properties. Understanding a material's optical constants, including optical band gap and extinction coefficient, is crucial for exploring its potential in optoelectronic applications.

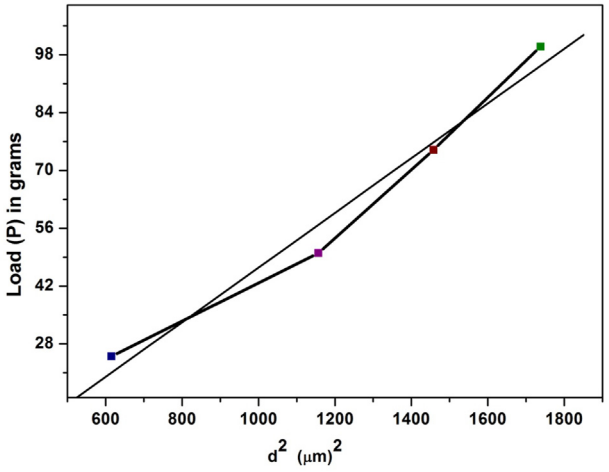

Fig. 6. Variation of d^2 vs load P for LLBC crystal.

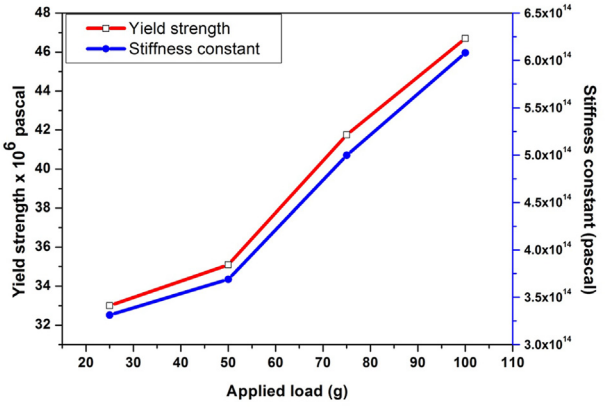

Fig. 7. Plot of change in yield strength and stiffness constant with applied load for LLBC.

"Using a UV-700 SHIMADZU spectrophotometer that operates in the 190−1100 nm wavelength range, LLBC's manufactured crystal conducted UV−visible spectroscopy investigation". A spectrophotometer is made up of a light source, a monochromator that separates radiation into its component wavelengths, a sample chamber, and a detector that measures how much light is transmitted by the sample. Fig. 8 displays the UV-visible transmittance spectrum of the LLBC crystal. The sample exhibits good transmittance in the visible region, with a lower cut-off wavelength of 224 nm. Fig. 9 illustrates the absorbance spectra of the LLBC crystal, indicating low absorbance in the visible region. The absorbance value was computed using the formula $\alpha = (1/t) \log10 (1/T)$, where T and t represent the sample's transmittance and thickness, respectively. Fig. 10 presents the variation of absorbance coefficient with wavelength for the LLBC crystal. These values of absorption coefficients are utilized to determine the optical energy gap, with the absorption coefficient (α) for photon energy following the relation (hv).

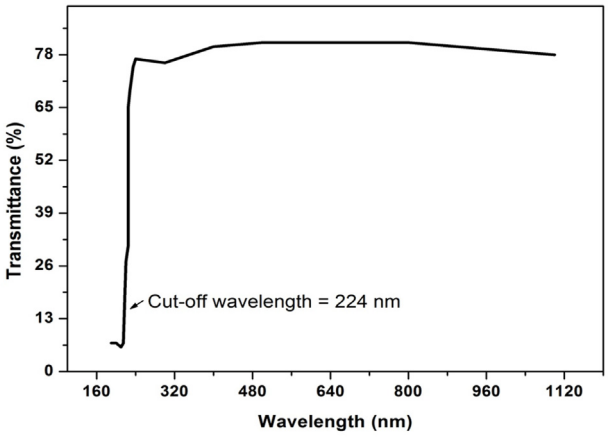

Fig. 8. Transmittance spectrum of LLBC.

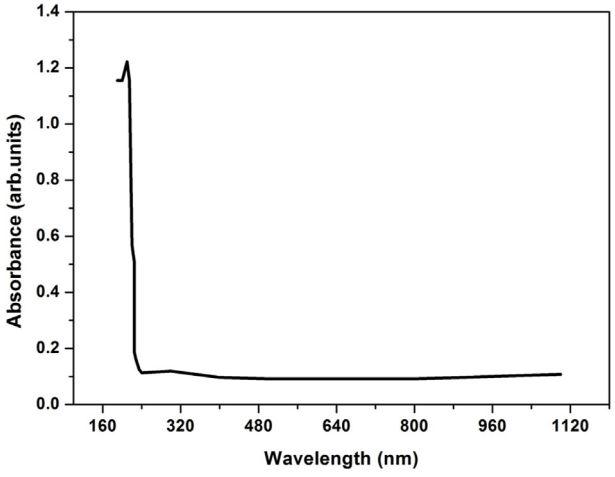

Fig. 9. Absorbance spectrum of LLBC.

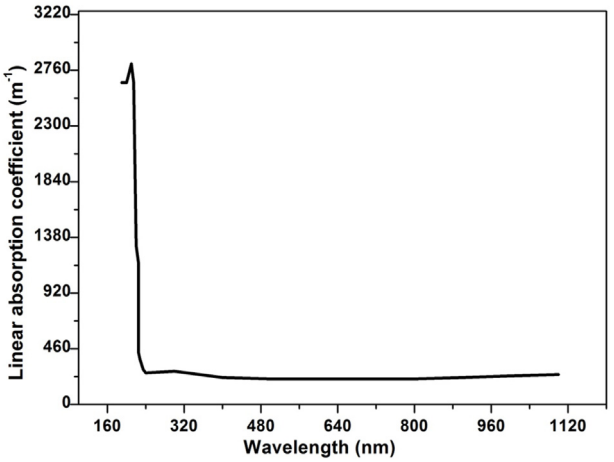

Fig. 10. Variation of absorption coefficient with wavelength for LLBC.

$$(\alpha\eta\gamma)^{\gamma} = A(\eta\gamma - E_{\gamma})$$

Where A is a constant and Eg is the optical band gap of the crystal. The Tauc plot of LLBC is produced by the above equation (Fig. 11). The type of transition is indicated by the value of the exponent "n" (for example, n = 12 for indirect transitions and n = 2 for direct transitions) [33]. The Tauc's figure yields the value of 5.51 eV for the LLBC crystal's optical band gap. LLBC crystal falls within the category of dielectrics due to its wide band gap.

The extinction coefficient (k) of the LLBC crystal was derived using the following connection.

$$K = \alpha\lambda/4\pi$$

where λ is the light's wavelength. The relationship between the sample's extinction coefficient and

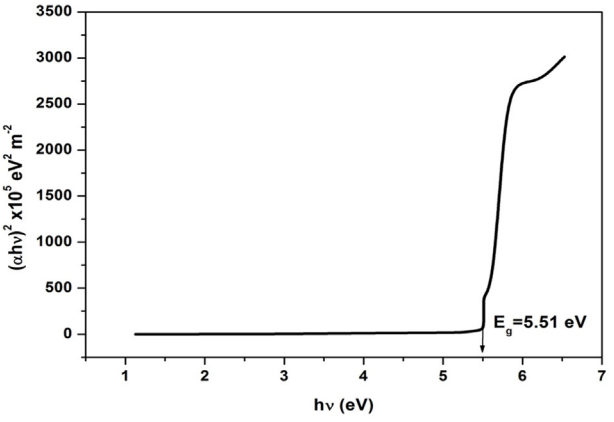

Fig. 11. Tauc's plot for LLBC.

wavelength is seen in Fig. 12. The results demonstrate that when wavelengths above the cut-off wavelength grow, the extinction coefficient increases. The crystal's low extinction coefficient value shows that there is little interaction between photons and electrons in the substance. Reflectance (R) measures how strongly a sample's surface reflects light. Reflectivity and reflectance coefficient are some of its other names. The reflectance reveals the energy proportion of light that is reflected to light that is incident on the sample. The reflectance was calculated using the subsequent expression [34].

$$R = 1 \pm (1 - e^{-\alpha t} + e^{\alpha t})^{1/2} \Big/ (1 + e^{-\alpha t})$$

where α is the absorption coefficient and t is the crystal's thickness. Fig. 13 shows how the LLBC crystal's reflectance varies with wavelength. The results demonstrate that the reflectance is high close to the UV cut-off wavelength and low in the visible region.

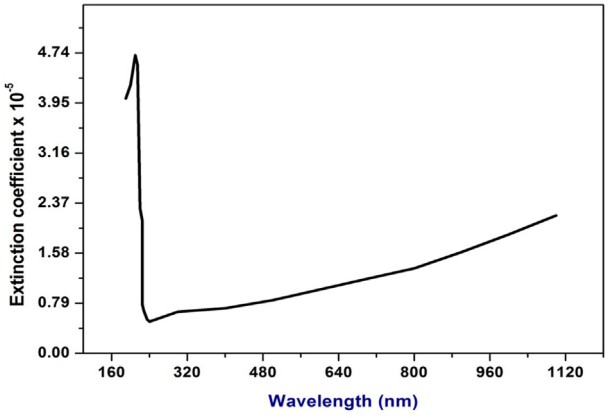

Fig. 12. Extinction coefficient vs wavelength for LLBC.

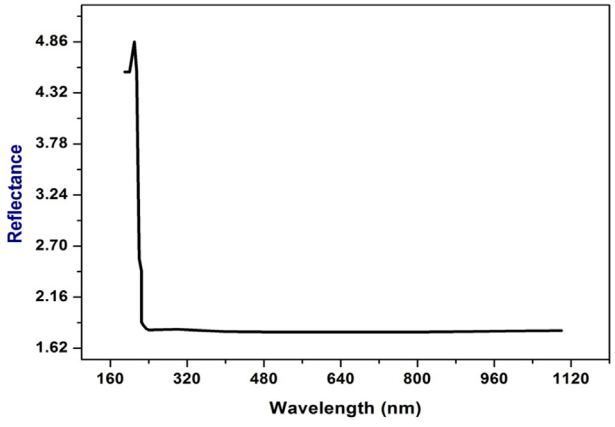

Fig. 13. Reflectance vs wavelength for LLBC.

Another linear optical property, the equation for linear refractive index (n), is given by

$$R\left[(n+1)^2 + k^2 = (n-1)^2 + k^2\right]$$

where the extinction factor is represented by k. In light of the fact that extinction coefficient (k) has a low value, we obtain

$$R = (n-1)^2 \Big/ (n+1)^2$$

The equation above can be used to get the linear refractive index of the LLBC crystal [35].

The variation of the refractive index with photon energy is shown in Fig. 14. As can be observed in the image, the refractive index is high at the forbidden band gap value and low in the visible range. The refractive index changes as the wavelength of the incident light beam changes due to the interaction between the photons and the crystal's composition. By varying the photon energy, we may create the desired material for the production of devices like electro-optic and optoelectronic ones. The optical conductivity of a substance is used to determine its frequency response when exposed to light.

The optical conductivity of the developed LLBC crystal was calculated using the following relationship.

$$\sigma_{opt} = \sigma nc / 4\pi$$

where n is the refractive index, α is the absorption coefficient, and c is the speed of light. Fig. 15 shows the relationship between the optical conductivity for LLBC crystals and wavelength. It is obvious that the refractive index and absorption coefficient of the material have an impact on the optical conductivity. It is evident that when the sample is close to the cut-off wavelength, its optical conductivity is strong. The LLBC crystal's

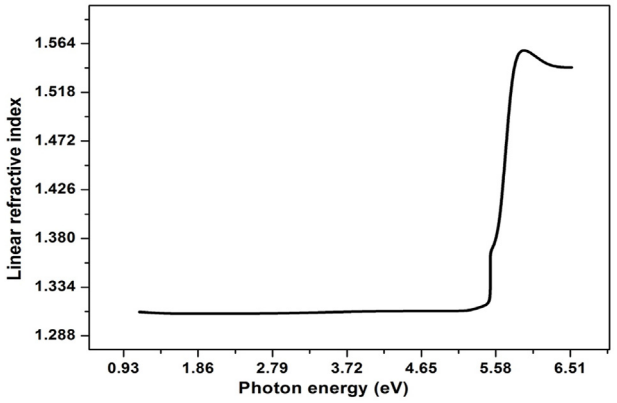

Fig. 14. Refractive index vs photon energy for LLBC.

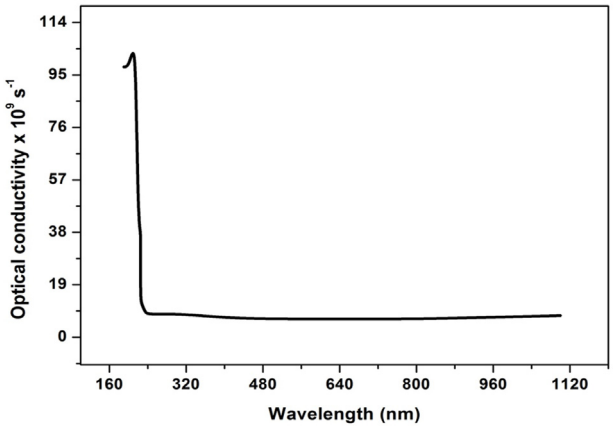

Fig. 15. Change of optical conductivity for LLBC as a function of wavelength.

high optical conductivity (10^9 s^{-1}) reveals that the material possesses high photo responsiveness.

"Electrical characteristics of LLBC crystals are described by their complex dielectric constant (c). A measure of the dissipation rate in the medium is provided by the imaginary component I of the complex dielectric constant, and information about dispersion is provided by the real part (r) of the dielectric constant, which is given by Ref. [36].

$$\varepsilon_c = (n + ik)^2$$

or $\varepsilon_c = n^2 - k^2 + i2nk$

where n is the refractive index and k is the extinction coefficient.

The real and imaginary parts of the dielectric constant are calculated using the following relationships:

$$\varepsilon_r = n^2 - k^2 \text{ and } \varepsilon_r = 2nk$$

Figures 16 and 17 show the variations of the real and imaginary components of the dielectric constant for the LLBC as a function of photon energy. The

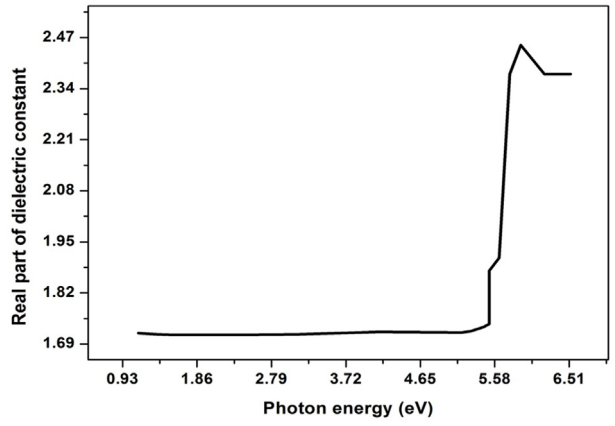

Fig. 16. Real part of the dielectric constant vs photon energy for LLBC.

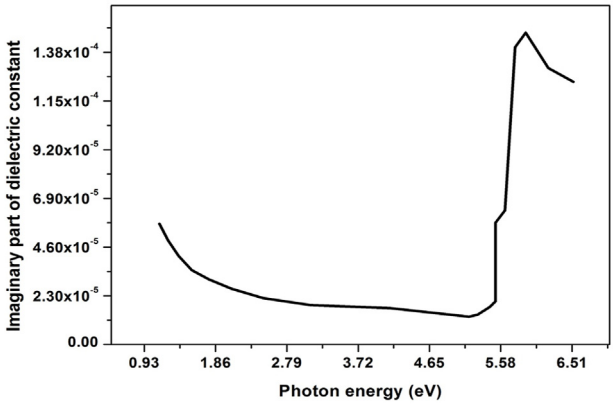

Fig. 17. Imaginary part of the dielectric constant vs photon energy for LLBC.

results show that the actual dielectric constant component is low, which qualifies the LLBC crystal for electro-optic applications. The imaginary part of the crystal's dielectric constant is where the dissipation factor, also known as dielectric loss, is related. As a result, LLBC crystal is of great quality and almost free of defects [37].

3.5. Antibacterial activity study

3.5.1. Samples of pathogenic bacteria

In this study, hazardous bacteria including *Staphylococcus aureus, Streptococcus*, *Klebsiella pneumoniae*, and *Pseudomonas aeruginosa* were used to examine the antibacterial activities of LLBC crystal.

3.5.2. Sub-culturing of bacterial strains

Sodium chloride, beef extract, yeast extract, peptic digest of animal tissue, and nutrient agar media were used to subculture the bacterial cultures. In order to preserve the bacterial culture for future investigation, it was maintained at 4 °C after a day of incubation at 37 °C.

3.5.3. Incubation of bacterial isolates

"*Streptococcus aureus*, *Klebsiella pneumoniae*, *Pseudomonas aeruginosa*, and *Streptococcus* were the four bacterial isolates that were chosen, and they were all grown independently in the basal medium". Basal medium (g/l) contains the following components: NaCl, glucose (0.5 g), yeast extract (0.1 g), peptone (0.25 g), KH2PO4 (0.05 g), and $MgSO_4$ (0.01 g) (1.0 g). The pH of the medium was adjusted to 7.0 by adding HCl/NaOH. After that, each isolate was given an injection, and it was incubated for 24 h at 37 °C. 50 ml of the culture media were added to 100 ml Erlenmeyer flasks for the experiment, which was then incubated at 30 °C for one day. After incubation, it was stored for upcoming investigation at 2−8 °C.

3.5.4. Antibacterial screening

The four bacterial strains used to assess the antibacterial efficacy of the created LLBC crystal were *Staphylococcus aureus, Streptococcus*, *Klebsiella pneumoniae*, and Pseudomonas aeruginosa. In an autoclave set at 121° Celsius for 15 min, the media, a pipette, Petri plates, and a metallic borer were all sterilised. After that, the culture media was put into sterile Petri plates. The disc was loaded with a 20 l LLBC sample, and activity was checked. 10 g of chloramphenicol served as the positive control (standard sample). Each plate underwent a 24-h incubation period at 37 °C, following which the diameter of the inhibition zone was measured in millimeters (mm) [38]. Fig. 18 shows schematics for a study on the antibacterial activity of certain substances. The measured zone of inhibition values are shown in Table 1. The results show that *Staphylococcus aureus* and *Pseudomonas aeruginosa* are more resistant to the LLBC crystalline sample's antibacterial action.

Table 1. Values of diameter of zone of inhibition for LLBC sample and standard sample against four bacterial pathogens.

Microorganism	Zone of inhibition	
	Standard	LLBC
S. aureus	20	32
Streptococcus sp.	20	10
Klebsiella pneumoniae	25	15
Pseudomonas aeruginosa	30	35

4. Conclusions

The L-Leucine Barium Chloride (LLBC) crystal was made by a slow evaporation process. It was found that the solubility of the material increased with temperature. The structure of LLBC was found to be orthorhombic. The relative SHG efficiency of the LLBC sample was 1.07 times higher than that of the KDP sample and this concludes that LLBC crystal can be applicable for laser and opto-electronic applications. The high mechanical strength of LLBC is shown to be a

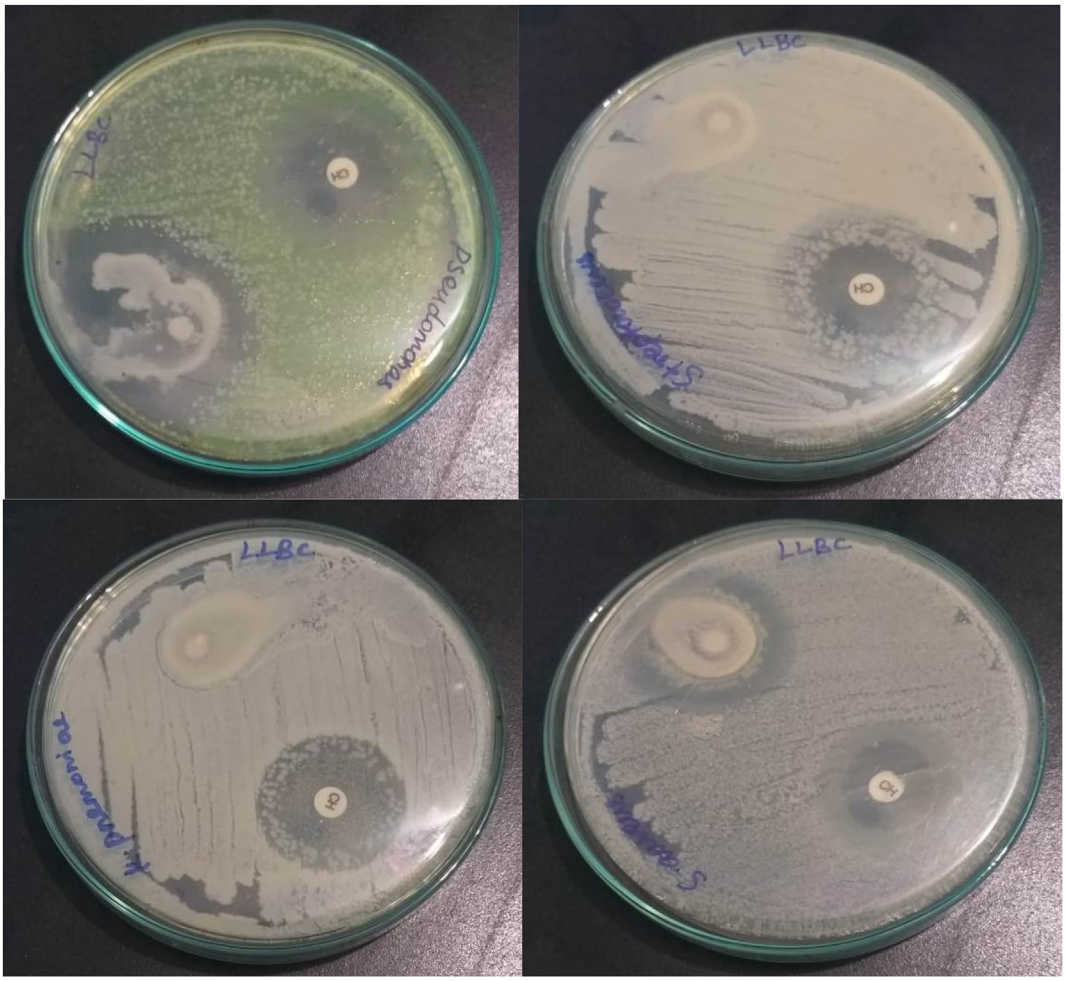

Fig. 18. Diagrams in connection with antibacterial activity study for LLBC crystalline sample against four bacterial strains.

result of its exceptional hardness. Microhardness investigations have been used to pinpoint the mechanical characteristics of LLBC. The sample has been shown to have a strong transmittance in the visible range, and an optical band gap measurement of 5.51 eV was made. The sample's optical conductivity is observed to be extraordinarily high, and the generated LLBC crystal's extinction coefficient is discovered to be exceedingly low. The real portion and imaginary part of the LLBC crystal's dielectric constant were calculated using refractive index and extinction coefficient values, and given their low values and the crystal's strong SHG efficiency, it is possible that NLO applications could benefit from the generated LLBC crystal. When the antibacterial activity of the LLBC sample was tested against four different bacterial strains, it was found that the sample was most effective against *Staphylococcus aureus* and *Pseudomonas aeruginosa* and hence this sample could be useful for medical applications.

Conflict of interest

The authors declare no competing interests.

Acknowledgments

Mrs. M. Arul Tresa (Reg, No: 18221282132038) is thankful to authorities of St. Xavier's College (Autonomous), Palayamkottai, Tirunelveli, and Manonmaniam Sundaranar University, Abishekapatti, Tirunelveli, Tamilnadu, India for providing necessary research facilities.

References

[1] D. Shanthi, et al., Optik 127 (2016) 3192.
[2] B.E. Umirzakov, et al., Eurasian J. Phys. Funct. Mater. 7 (2023) 249.
[3] B. Sahaya Infant Lasalle, Muthu Senthil Pandian, K. Anitha, P. Ramasamy, Inorg. Chem. Commun. 157 (2023) 111397.
[4] I. Johnson Alexandar, A. Maggie Dayana, T.C. Sabari Girisun, B. Sahaya Infant Lasalle, Muthu Senthil Pandian, Inorg. Chem. Commun. 159 (2024) 111751.
[5] Raman Arunpandian, B. Sahaya Infant Lasalle, N. Balagowtham, Moorthy Krishnamachari, Muthu Senthil Pandian, A. Alexandar, J. Mol. Struct. 1288 (2023) 135811.
[6] B. Sahaya Infant Lasalle, Pandian Muthu Senthil, P. Karuppasamy, Ramasamy P. Gunasekaran, Inorg. Chem. Commun. 158 (2023) 111549.
[7] S. Adhikari, T. Kar, Mater. Chem. Phys. 133 (2012) 1055.
[8] M. Kh Balapanov, et al., Eurasian J. Phys. Funct. Mater. 1 (2017) 40.
[9] M. Anbuvhezhiyan, et al., Optoelectron. Adv. Mat. Rapid Commun 3 (2009) 1161.
[10] M.K. Marchewka, M. Drozd, Cent. Eur. J. Chem. 11 (B) (2013) 1264.
[11] G. Bhagavannarayana, et al., Mater. Chem. Phys. 126 (2011) 20.
[12] M.R. Jagadeesh, et al., Mater. Sci.-Pol. 33 (2015) 529.
[13] P. Baskaran, et al., J. Taibah Univ. Sci. 11 (2017) 11.
[14] S. Guidara, et al., Spectrochim. Acta Part A 115 (2013) 437.
[15] G. Bhagavannarayana, et al., Mater. Chem. Phys. 126 (2012) 20.
[16] P. Baskaran, et al., Arch. Appl. Sci. Res. 6 (2014) 90.
[17] J. Janczak, G.J. Perpetuo, Acta Crystallogr. Sect. C: Cryst. Commun. 63 (2007) o117.
[18] M. Anbuchezhiyan, S. Ponnusamy, C. Muthamizhchelvan, Optoelectron. Adv. Mater. Rapid Commun. 3 (2009) 1161−1167.
[19] P. Baskaran, S. Rajasekar, M. Kumar, M. Vimalan, K. Selvaraju, Arch. Appl. Sci. Res. 6 (2014) 90−98.
[20] S. Adhikari, T. Kar, Mater. Res. Bull. 48 (2013) 1612−1617.
[21] E. Subramanian, Acta Cryst. 22 (1967) 910−917.
[22] Sameh Guidara, Feki Habib, Younes Abid, Spectrochim. Acta, Part A A115 (2013) 437−444.
[23] G. Bhagavannarayana, B. Riscob, Mohd Shakir, Mater. Chem. Phys. 126 (2012) 20−23.
[24] Soma Adhikari, Tanusree Kar, J. Cryst. Growth 356 (2012) 4−9.
[25] Janczak Jan, Genivaldo Julio Perpetuo, Acta Cryst. C63 (2007) o117−o119.
[26] S.K. Kurtz, T.T. Perry, J. Appl. Phys. 39 (1968) 3798.
[27] J. Bowman, M. Bevis, Prog. Colloid Polym. Sci. 255 (1977) 954.
[28] J.R. Pandya, et al., Bull. Mater. Sci. 5 (1983) 79.
[29] R. Asok Kumar, et al., Sch. Res. Lib. 2 (2010) 247.
[30] C. Hays, E.G. Kendall, Metallography 6 (1973) 275.
[31] W.A. Wooster, Rep. Prog. Phys. 16 (1953) 62.
[32] B.R. Lawn, E.R. Fuller, J. Mater. Sci. 10 (1975) 2016.
[33] S. Krishnan, et al., Cryst. Res. Technol. 43 (2008) 670.
[34] R. Hanumantharao, et al., Spectrochim. Acta Part A 91 (2012) 345.
[35] D.P. Gosain, et al., J. Mater. Sci. 26 (1991) 3271.
[36] G. Marudhu, et al., Optik 125 (2014) 2417.
[37] P. Selvarajan, et al., J. Mater. Sci. 29 (1994) 4061.
[38] G.G.F. Nascimento, et al., Braz. J. Microbiol. 31 (2000) 886.